18th AIAA/CEAS Aeroacoustics Conference (33rd AIAA Aeroacoustics Conference)
04 - 06 June 2012, Colorado Springs, CO
AIAA 2012-2159

Aeroacoustics of Three-Stream Jets

Brenda Henderson*
NASA Glenn Research Center, Cleveland, OH

Results from acoustic measurements of noise radiated from a heated, three-stream, co-annular exhaust system operated at subsonic conditions are presented. The experiments were conducted for a range of core, bypass, and tertiary stream temperatures and pressures. The nozzle system had a fan-to-core area ratio of 2.92 and a tertiary-to-core area ratio of 0.96. The impact of introducing a third stream on the radiated noise for third-stream velocities below that of the bypass stream was to reduce high frequency noise levels at broadside and peak jet-noise angles. Mid-frequency noise radiation at aft observation angles was impacted by the conditions of the third stream. The core velocity had the greatest impact on peak noise levels and the bypass-to-core mass flow ratio had a slight impact on levels in the peak jet-noise direction. The third-stream jet conditions had no impact on peak noise levels. Introduction of a third jet stream in the presence of a simulated forward-flight stream limits the impact of the third stream on radiated noise. For equivalent ideal thrust conditions, two-stream and three-stream jets can produce similar acoustic spectra although high-frequency noise levels tend to be lower for the three-stream jet.

I. Introduction

FUTURE turbine-engine architectures may provide a third exhaust stream that will be available for potential noise reduction technologies. Using the third stream as an additional bypass stream allows for the reduction of the velocity shear rate between the bypass flow and the ambient air and may also allow for alteration of the core and bypass velocities while maintaining thrust, thus allowing for reduced velocity shear rates between the core and bypass flows as well. However, the noise characteristics (and potential noise reduction) of three-stream jets are unknown. The current study investigates the noise characteristics of a heated, three-stream, co-annular jet operated at subsonic exhaust conditions.

System studies that investigate the trades between performance and noise for future supersonic aircraft will need noise prediction tools for three-stream jets. Current predictive tools address single[1,2,3] and dual-stream[1,4,5] jets. To apply these tools to three-stream jets, it is necessary to assume that two of the three jet streams are fully mixed, an assumption that may be inadequate for some future engine exhausts. Previous three-stream experiments focused on using the third stream to reduce the shearing rate at the outer flow boundary and modify the jet shock structure in an inverted-velocity-profile, supersonic, dual-stream jet[6]. Subsonic exhaust conditions were not investigated. The development of new semi-empirical prediction tools will require the acquisition of relevant noise databases that can be used for model development, calibration, and validation. These databases do not exist so extension of existing prediction tools or the development of new tools is not currently possible.

The purpose of the work reported here is to investigate the noise characteristics of a three-stream exhaust system with nozzle area ratios similar to those that may be used for future supersonic commercial aircraft. The study focuses on subsonic jet exhausts as future, supersonic, commercial aircraft will have takeoff engine exhausts that are at high subsonic or low supersonic speeds. The study will include the impact of jet velocities, jet velocity ratios, and forward flight on far-field noise.

II. Experimental Approach

The experiments were conducted in the Aero-Acoustic Propulsion Laboratory (AAPL) at the NASA Glenn Research Center shown in Fig. 1. The AAPL is a 66 ft radius geodesic dome treated with acoustic wedges. The AAPL contains the Nozzle Acoustic Test Rig (NATR), which produces a 53 inch diameter simulated forward-flight stream reaching Mach numbers of 0.35. The High Flow Jet Exit Rig (HFJER), a dual-stream jet engine simulator capable of replicating most commercial turbo-fan engine temperatures and pressures [see Ref. (7)], is centered in the

* Researcher, Acoustics Branch, MS 54-3, 21000 Brookpark Rd., Cleveland, OH 44135.

simulated flight stream of the NATR. A third-stream capable of achieving mass-flow rates between 0.5 – 6 lbm/sec has been added to the HFJER. The third-stream flow temperatures are equal to that of the bypass stream as the former stream branches off the latter stream after the bypass heater.

The three-stream nozzle system used in the experiments is shown in Fig. 2. The round core nozzle is shown in Fig. 2 (a) and the core lobed-mixer nozzle is shown in Fig. 2 (b). The exit diameter of the core nozzle is 4.8 in. The fan-to-core area ratio at the core nozzle trailing edge is 2.92 and the tertiary-to-core area ratio 0.96. Nozzle areas were calculated at the nozzle trailing edges. The area ratios remained constant throughout the experiments.

Acoustic measurements were made with the far-field array shown in Fig. 1. The array contains 24 microphones located on a 45 foot constant radius arc covering polar angles between 45^o and 160^o, where angles greater than 90^o are in the downstream direction relative to the third-stream nozzle exit. All data were corrected for atmospheric absorption[8] and wind tunnel shear layer effects[9] and are presented on a one-foot lossless arc. Data are acquired using ¼" Bruel and Kjaer microphones (without protection grids) pointed directly at the nozzle exit. Microphone sensitivity and frequency response have been applied to all measurements. Narrowband data were acquired in 12 Hz bands and results are presented as power-spectral density (PSD).

The conditions used in the experiments are shown in Table 1. The Nozzle Pressure Ratio, NPR, is the ratio of the stagnation pressure of the indicated stream to the ambient pressure. Subscripts "c", "b", and "t" indicate the core, fan, and tertiary streams, respectively. The subscript "a" indicates ambient conditions. The nozzle temperature ratio (NTR), is the ratio of the stagnation temperature of the indicated stream to the ambient temperature. The quantity M_{fj} is the free jet (simulated flight stream) Mach number. All data were acquired for $NTR_b = 1.25$. Stagnation temperature measurements in the third stream indicated that the third-stream temperature was equal to that of the bypass flow. The cycle points were selected to obtain a range of mass-flow rates, stream velocities, and velocity ratios. Velocities (V), mass-flow rates (W), speed of sound (c), velocity ratios, and mass-flow ratios for the conditions presented here are shown in Table 2. The reported thrust results for the nozzle system are ideal and are calculated from measured flow rates and ideal velocities obtained from isentropic calculations. Note that mass flow rates are impacted when the core and bypass pressures are not matched due to the fact that the higher pressure stream slightly cuts off the flow of the lower pressure stream.

III. Results

Three-stream results are compared to results from the baseline (three-stream) experiment in which $NPR_c = NPR_b = 1.8$, $NTR_c = 3.2$, $1.0 \leq NPR_t \leq 1.8$, and $M_{fj} = 0.0$. Jet conditions with $NPR_t = 1.0$ and 1.8 are intended to simulate those for dual-stream jets with different bypass-to-core mass-flow ratios. However, the three-stream exhaust will not exactly replicate the flow from dual-stream nozzles due to the fact that the third stream nozzle will alter ambient air entrainment for $NPR_t = 1.0$. Additionally, for $NPR_t = 1.8$, the nozzle boundary layers will transition to a shear layer between the bypass and third-stream flows that will persist for a short distance downstream of the nozzle trailing edges. Results are first presented for the baseline experiments then the impact of changing the core velocity, bypass velocity, and bypass-to-core mass flow ratio on the resulting noise are investigated. The impact of simulated forward flight on the acoustic radiation from three-stream jets is also presented. Finally, comparisons between the noise radiated from the three-stream exhaust system and a simulated two-stream jet are made on an equal thrust basis. Results are presented for the round core nozzle unless otherwise stated.

A typical repeatability result for data acquired during the experiments is shown in Fig. 3. The data have been smoothed by shifting the value of each point to an average value determined from neighboring points. The impact of smoothing the data is shown in Fig. 4. In the plot legend, the three-number designation corresponds to NPR_c, NPR_b, and NPR_t. As shown in the Figs. 3 and 4, the data scatter within each band is no greater that ½ dB.

Results for the baseline experiment are shown in Figs. 5. The bypass-to-core velocity ratio for all data in Fig. 5 is 0.62 (see Table 2). As shown in Fig. 5(a), results for $NPR_t = 1.0$ and 1.8 are similar for a 90^o observation angle. Introducing the third stream at a velocity lower than that of the bypass stream (NPR_t equal to 1.3 or 1.5) reduces mid and high frequency acoustic levels for frequencies greater than 4000 Hz. In the peak jet noise direction (150^o), acoustic levels at mid frequencies (2000 Hz – 5000 Hz) decrease with increasing third-stream pressure. At high frequencies (above 7000 Hz), acoustic levels are the same for $NPR_t = 1.0$ and $NPR_t = 1.8$ most likely due to the fact that the noise is dictated by the outer-most shear layer that remains unchanged for $NPR_t = 1.0$ and 1.8. For $NPR_t = 1.3$ and 1.5, high frequency noise is reduced relative to that for $NPR_t = 1.0$ (and 1.8) which is likely due to the reduced velocity ratio between the third and ambient streams. Tones occurring at very high frequencies (70,000 – 80,000 Hz) are trailing edge tones caused by vortex shedding from the fan/core nozzle trailing edge which can occur for velocity ratios greater than 0.6 [see Ref. 10]. Differences in the power-spectral-density levels (designated "Delta PSD") relative to the jet with $NPR_t = 1.0$ are shown in Fig. 6 for the jet conditions in Fig. 5. Delta PSD is positive

when the three-stream jet (or simulated two stream jet with $NPR_t = 1.8$) has an acoustic level lower than that for $NPR_t = 1.0$. For $NPR_t = 1.3$ or 1.5 and an observation angle of 90^o, a reduction of 2 dB is achieved with the three-stream jet relative to the simulated two stream jets ($NPR_t = 1.0$ or 1.8) at frequencies near 30,000 Hz. In the peak jet noise direction, a maximum mid-frequency reduction of 3.5 dB is achieved for $NPR_t = 1.5$ and high frequency (greater than 10,000 Hz) reduction of 3 dB for $NPR_t = 1.3$ relative to the acoustic levels for $NPR_t = 1.0$. Peak noise levels at both observation angles are unaffected by third-stream jet conditions.

The results obtained for the three-stream jet at reduced core and bypass pressures (and velocities) and the same core-to-bypass velocity ratio as that used in the baseline experiments are shown in Figs. 7 and 8. The impact of the third stream on the radiated noise is similar to that found in the previous set of data (baseline experiment) although the peak noise reduction (relative to $NPR_t = 1.0$) in the peak jet-noise direction is slightly greater for the lower pressure core and bypass streams than for the higher pressure core and bypass streams [see Figs. 8(b) and 6 (b), respectively]. The third stream conditions have a greater impact on high-frequency noise levels in the peak jet-noise direction for the baseline experiments than for the conditions in Fig. 8 due to the fact that the fan-to-ambient flow velocity ratio is lower for the jet conditions in Fig. 8 (b) than for the conditions in Fig. 6(b). Peak noise levels were unaffected by the third stream conditions.

The impact of introducing a third stream at a bypass-to-core velocity ratio greater than that of the baseline experiments is shown in Figs. 9 and 10. An increase in bypass-to-core velocity ratio was achieved by reducing the core pressure (and velocity). The results for $NPR_t = 1.5$ have been omitted from Fig. 9 for clarity. As indicated in Table 2, the bypass-to-core mass-flow ratio (W_b/W_c) has decreased from 4.7 for the baseline experiments to 4.3 for the conditions shown in Figs. 9 and 10. The impact of the third stream on the radiated noise is similar to that observed in the baseline experiments although high-frequency noise reduction in the peak jet-noise direction for $NPR_t = 1.3$ (relative to $NPR_t = 1.0$) is lower for the increased fan-to-core velocity ratio than for the lower fan-to-core velocity ratio used in the baseline experiments.

The results obtained from introducing a third stream at a reduced bypass-to-core velocity ratio achieved by reducing the bypass pressure (and velocity) relative to that used in the baseline experiments are shown in Figs. 11 and 12. Reducing the bypass-to-core velocity ratio had the impact of reducing the shearing rates between the bypass and third streams relative to the baseline experimental conditions using the same NPR_t.. While peak levels are not affected by the introduction of the third stream, acoustic levels at all frequencies greater than the peak frequencies are reduced (relative to $NPR_t = 1.0$) for both observation angles when NPR_t is equal to 1.3 or 1.5. For a 90^o observation angle, a peak noise reduction (relative to the simulated two-stream jets with $NPR_t = 1.0$ and 1.8) of 3 dB is achieved with $NPR_t = 1.3$. In the peak jet-noise direction, the maximum reduction at mid-frequencies (5000 Hz) is 3.5 dB for $NPR_t = 1.5$ and maximum high-frequency (above 10,000 Hz) reduction is 3 dB for $NPR_t = 1.3$.

The spectra in Fig. 13 show the impact of reducing the core velocity [Fig. 13 (a)], the bypass velocity [Fig. 13 (b)], and the bypass-to-core mass-flow ratio [Fig. 13 (c)] on the noise radiated from three-stream jets. Reducing the core-stream velocity while maintaining the bypass and third stream velocities [$NPR_c = 1.7$, $NPR_b = 1.8$, and $NPR_t = 1.3$ in Fig. 13 (a)] reduces the acoustic levels at all frequencies for broadside and peak jet-noise observations angles. Reducing the bypass velocity while maintaining core and tertiary stream velocities [$NPR_c = 1.8$, $NPR_b = 1.7$, and $NPR_t = 1.3$ in Fig. 13 (b)] has little impact on the radiated noise. Reducing the bypass-to-core mass-flow ratio while maintaining the core, bypass, and third stream velocities [$NPR_c = 1.8$, $NPR_b = 1.8$, and $NPR_c = 1.3$ in Fig. 13 (c)] slightly increases the acoustic levels at low frequencies for broadside observation angles and all frequencies in the peak jet noise direction.

The noise characteristics for a three-stream jet in a Mach 0.3 simulated flight stream are shown in Figs. 14 and 15. The jet conditions are the same as those used in the baseline experiments. At a broadside angle to the jet, slight reductions in noise above 5000 Hz are achieved for NPR_t equal to 1.3 or 1.5 (relative to noise levels for $NPR_t = 1.8$). Low frequency levels are the same for all three-stream jets and the simulated two-stream jet with $NPR_t = 1.8$. In the peak jet-noise direction, the lowest acoustic levels for frequencies below 10,000 Hz are achieved for the simulated two-stream jet where the third stream is operated at the same conditions as the bypass. Little high frequency noise reduction is achieved with the three-stream jets which is likely due to the fact that the velocity differences between the third stream and the flight stream are greatly reduced for the conditions in Figs. 14 and 15 relative to those in Figs. 5 and 6. A comparison of the results in Figs. 5 and 6 with those in Figs. 14 and 15 indicate that noise reduction predictions based on third-stream jets at static free jet conditions will be overly optimistic when applied to three-stream jets with simulated or real forward flight.

The noise characteristics associated with partially mixed three-stream jets are shown in Fig. 16. For these experiments, the round core nozzle was replaced by the core lobed-mixer nozzle shown in Fig. 2 (b). Preliminary particle image velocimetry results indicated that the bypass and core flows were not fully mixed at the trailing edge of the nozzle system. For a 90^o observation angle, the spectra for all third-stream conditions are similar to those for

both simulated two-stream jets for frequencies below 10,000 Hz. For frequencies above 10,000 Hz, the acoustic levels for both three-stream jets are close to those for the simulated two-stream jet with $NPR_t = 1.06$. In the peak jet noise-direction, the third-stream conditions only impacted high frequency noise, and reductions (relative to $NPR_t = 1.06$ or 1.8) in this region of the spectra were limited.

The data shown in Figs. 17 and 18 were acquired at equal ideal thrust conditions. For Fig. 17, results for a three-stream jet are compared with those from a simulated two-stream jet at $NPR_c = NPR_b = NPR_t = 1.7$. At a 90^o observation angle, the acoustic levels for the simulated two-stream jet are nearly identical to those obtained for the three-stream jet. In the peak jet noise direction, acoustic levels at frequencies below 1700 Hz are lower for the two-steam jet than for the three-stream jet. For frequencies above 6500 Hz, acoustic levels are lower for the three-stream than the simulated two-stream jet. In Fig. 18, results for a three-stream jet are compared with those from a simulated two-stream jet achieved by shutting off the third-stream flow ($NPR_t = 1.0$). The bypass ratios for both jet exhausts are equal but the core velocity is higher for the simulated two-stream jet than for the three-stream jet. The acoustic levels at all frequencies at both observation angles are lower for the three-stream jet than the simulated two-stream jet. The differences in the acoustic levels for the two jet exhausts in Fig. 18 are likely due to differences in core velocities. The data in Figs. 17 and 18 indicate that three-stream jets (at the area ratios investigated here) are not inherently quieter than two-stream jets when compared on an equal thrust basis. However, the presence of the third stream may allow for the reduction of the core-stream velocity while maintaining thrust which will impact radiated noise.

IV. Discussion and Conclusions

The acoustic radiation characteristics of three-stream jets were investigated. The addition of a third stream to a simulated two-stream jet reduced high-frequency acoustic radiation at broadside and peak jet-noise angles for a static free jet. Mid-frequency acoustic levels are also impacted by the presence of the third stream. In the presence of a simulated flight stream, the addition of the third stream had a reduced impact on the radiated noise relative to that achieved with a static flight stream. Reducing the core stream velocity had a greater impact on the radiated noise than reducing the fan stream velocity or reducing the bypass-to-core mass flow ratio. Comparisons made on an equal thrust basis showed that the three-stream jet did not have inherently lower acoustic levels than a two-stream jet. However, the addition of a third stream may allow for more flexibility in selecting a cycle that will meet performance and noise requirements.

The experiments reported here used a nozzle system with constant area ratios so it was not possible to determine the impact of the third stream over a range of bypass-to-core and bypass-to-tertiary area ratios. Additional experiments that allow for the variation of area ratios will need to be pursued to fully understand the noise characteristics of three-stream jets.

Acknowledgement

The hardware used in the experiments was designed and manufactured by Rolls-Royce under Supersonics Project NRA NNC10CA02C. This work was supported by the Supersonics Project in the Fundamental Aeronautics Program.

References

[1]Gillian, R. E., Aircraft Noise Prediction Program User's Manual, NASA Langley Research Center, 1982.
[2]Tam, C. K. W., Golebiowski, M., and Seiner, J. M. "On the two components of turbulent mixing noise from supersonic jets," AIAA-1996-1716, 1996.
[3]Viswanathan, K. "Improved method for prediction of noise from single jets," AIAA J. Vol. 45, No. 1, 2007, pp. 151-161.
[4]Stone, J. R., Groesbeck, D. E., and Zola, C. L. "An improved prediction method for noise generated by conventional profile coaxial jets," AIAA 81-1991, Palo Alto, CA, 1991.
[5]Khavaran, A. and Bridges, J. "Jet noise scaling in dual stream nozzles," AIAA-2010-3968, 2010.
[6]Soeder, R., Wnuk, S., and Loew, R. "Aero-Acoustic Propulsion Laboratory Nozzle Acoustic Test Rig User Manual," NASA/TM-2006-212939, 2006.
[7]Dosanjh, D. S. "flow and noise characteristics of multi-stream coaxial supersonic jets," AIAA-81-1977, 1981.
[8]ANSI S1.26-1995 (R2004), "Method for calculation of absorption of sound by the atmosphere".
[9]Amiet, R. K., "Correction of open jet wind tunnel measurements for shear layer refraction," AIAA-77-54, 1977.
[10]Henderson, B., Kinzie, K., and Haskin, H. "The effect of nozzle trailing edge thickness on jet noise," AIAA 2004-2948, 2004.

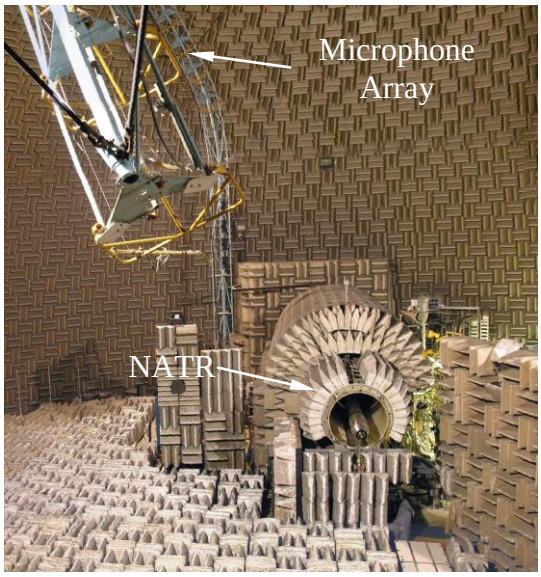

Figure 1. A photograph of the Aero-Acoustic Propulsion Laboratory (AAPL) showing the Nozzle Acoustic Test Rig (NATR).

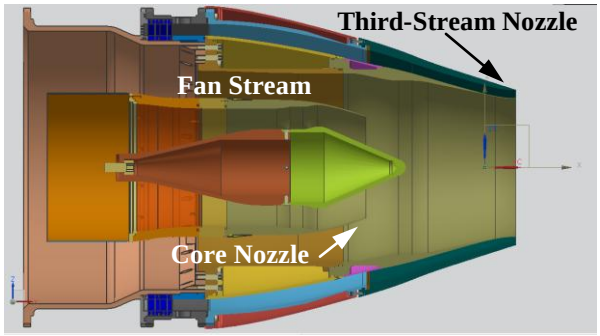

(a)

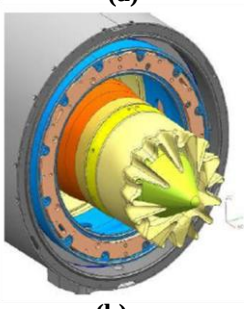

(b)

Figure 2. The three-stream nozzle system used in the experiments.

Table 1 Experimental Conditions

NPR_c	NPR_b	NPR_t	NTR_c	$M_{fj} = 0$	$M_{fj} = 0.2$	$M_{fj} = 0.3$
1.5	1.5	1.0 - 1.5	2.8	✓		
1.6	1.6	1.0 - 1.6	2.8	✓		
1.7	1.7	1.0 - 1.7	2.8	✓		
1.8	1.8	1.0 - 1.8	2.8	✓		
1.5	1.5	1.0 - 1.5	3.2	✓		
1.5	1.4	1.0 - 1.4	3.2	✓		
1.5	1.6	1.0 - 1.6	3.2	✓		
1.6	1.5	1.0 - 1.5	3.2	✓		✓
1.6	1.6	1.0 - 1.6	3.2	✓		✓
1.6	1.7	1.0 - 1.7	3.2	✓		✓
1.7	1.6	1.0 - 1.6	3.2	✓	✓	✓
1.7	1.7	1.0 - 1.7	3.2	✓	✓	✓
1.7	1.8	1.0 - 1.8	3.2	✓	✓	✓
1.8	1.7	1.0 - 1.7	3.2	✓		✓
1.8	1.8	1.0 - 1.8	3.2	✓	✓	✓

Table 2 Jet Exhaust Conditions

NPR_c	NPR_b	NPR_t	NTR_c	V_c (ft/s)	V_b (ft/s)	V_t (ft/s)	C_c (ft/s)	C_b (ft/s)	C_t (ft/s)	C_a (ft/s)	W_c (lbm/s)	W_b (lbm/s)	W_t (lbm/s)	Ideal Thrust (lbf)	V_b/V_c	V_t/V_b	W_b/W_c
1.6	1.6	1.3	2.8	1470	978	740	1710	1154	1177	1107	3.3	14.4	3.4	680	0.67		4.4
1.7	1.7	1.0	2.8	1561	1036		1700	1144		1107	3.6	15.6		688	0.66		4.3
1.7	1.7	1.7	2.8	1561	1036	1036	1700	1144	1139	1107	3.6	15.6	5.1	854	0.66	1.00	4.3
1.8	1.8	1.0	2.8	1633	1085		1685	1135		1107	3.9	16.6		769	0.66		4.3
1.8	1.8	1.3	2.8	1633	1085	737	1685	1135	1179	1107	3.9	16.6	3.4	853	0.66	0.68	4.3
1.8	1.8	1.5	2.8	1633	1085	910	1685	1135	1157	1107	3.9	16.6	4.4	891	0.66	0.84	4.3
1.8	1.8	1.8	2.8	1633	1085	1081	1685	1135	1130	1107	3.9	16.6	5.5	950	0.66	1.00	4.3
1.5	1.5	1.0	3.2	1480	916		1848	1170		1113	2.8	12.9		510	0.62		4.6
1.5	1.5	1.3	3.2	1480	916	730	1848	1170	1177	1113	2.8	12.9	3.4	588	0.62	0.80	4.6
1.5	1.5	1.5	3.2	1480	916	911	1848	1170	1156	1113	2.8	12.9	4.4	637	0.62	0.99	4.6
1.6	1.6	1.3	3.2	1575	980		1816	1150	1173	1105	3.0	14.1		664	0.62	0.00	4.7
1.7	1.8	1.3	3.2	1667	1084	733	1808	1133	1178	1106	2.8	16.9	3.3	814	0.65	0.68	6.0
1.7	1.8	1.5	3.2	1662	1084	906	1808	1133	1155	1106	2.8	17.0	4.3	855	0.65	0.84	6.1
1.8	1.7	1.0	3.2	1750	1038		1800	1143		1108	4.0	14.9		716	0.59		3.7
1.8	1.7	1.3	3.2	1750	1038	738	1800	1145	1178	1108	4.0	14.9	3.4	793	0.59	0.71	3.7
1.8	1.7	1.5	3.2	1750	1038	911	1800	1145	1156	1108	4.0	14.9	4.4	835	0.59	0.88	3.7
1.8	1.7	1.7	3.2	1750	1038	1031	1800	1145	1138	1108	4.0	14.9	5.1	878	0.59	0.99	3.7
1.8	1.8	1.0	3.2	1750	1085		1799	1135		1107	3.5	16.6		774	0.62		4.7
1.8	1.8	1.3	3.2	1750	1085	739	1799	1135	1181	1107	3.5	16.6	3.4	856	0.62	0.68	4.7
1.8	1.8	1.5	3.2	1750	1085	909	1796	1135	1159	1107	3.5	16.6	4.4	898	0.62	0.84	4.7
1.8	1.8	1.8	3.2	1750	1085	1083	1797	1135	1129	1107	3.5	16.6	5.5	954	0.62	1.00	4.7

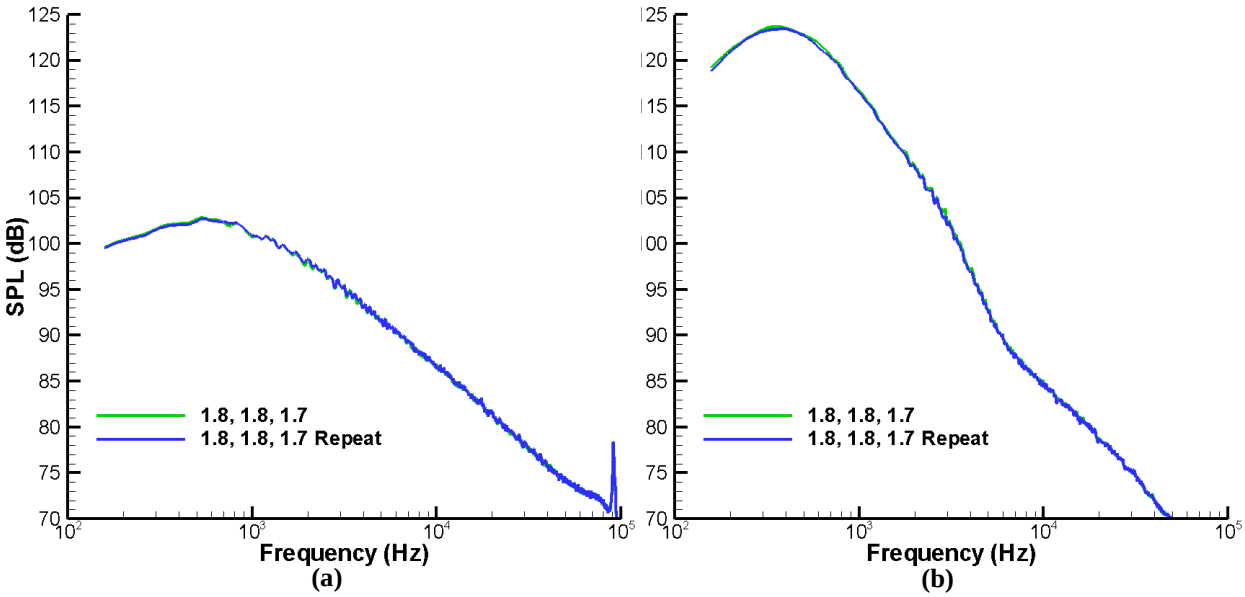

Figure 3. Narrowband data acquired at NTR_c = 3.2, M_{fj} = 0.3, and the indicated NPRs for observation angles equal to (a) 90° and (b) 150°.

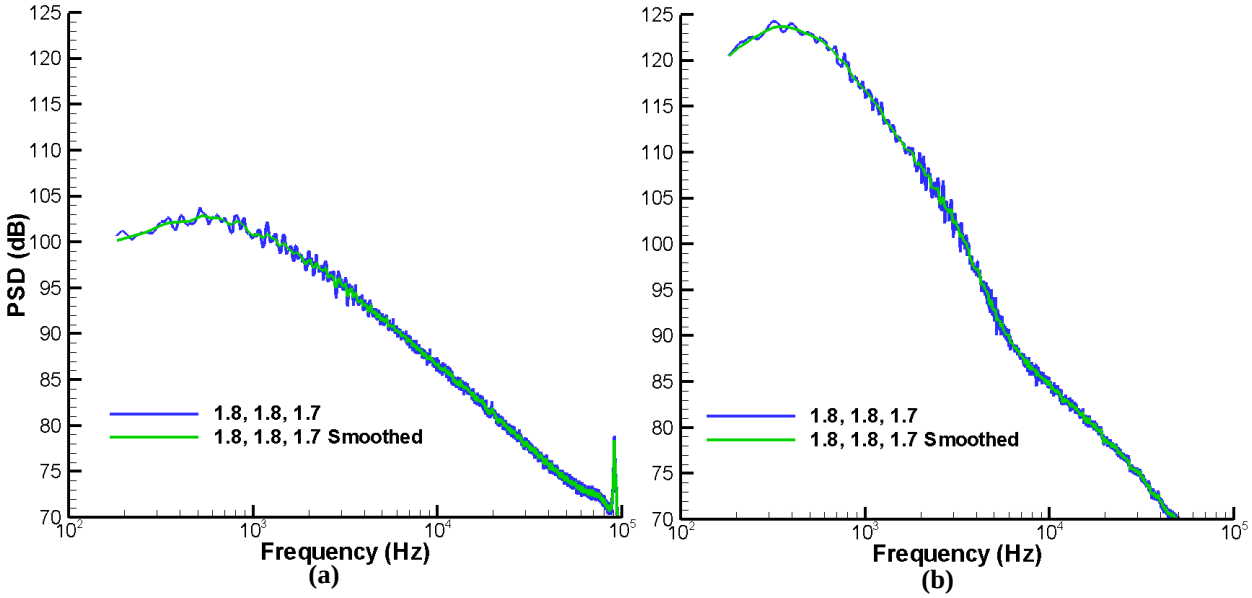

Figure 4. Narrowband data acquired at NTR_c = 3.2, M_{fj} = 0.3, and the indicated NPRs for observation angles equal to (a) 90° and (b) 150°.

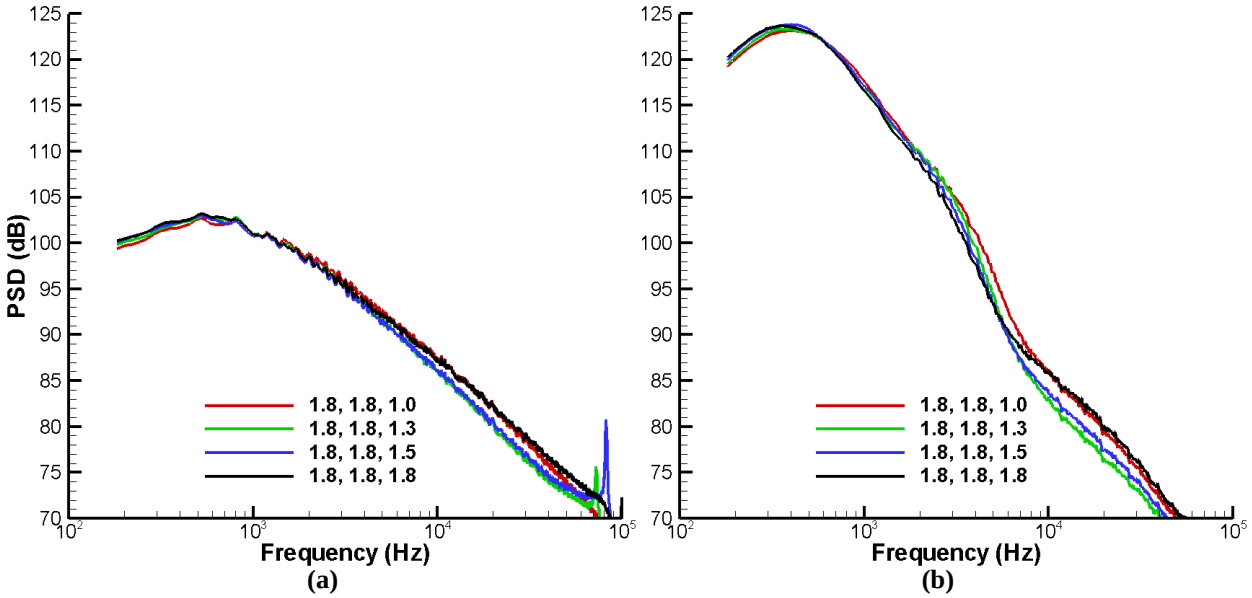

Figure 5. Narrowband data acquired at NTR_c = 3.2, M_{fj} = 0, and the indicated NPRs for observation angles equal to (a) 90° and (b) 150°.

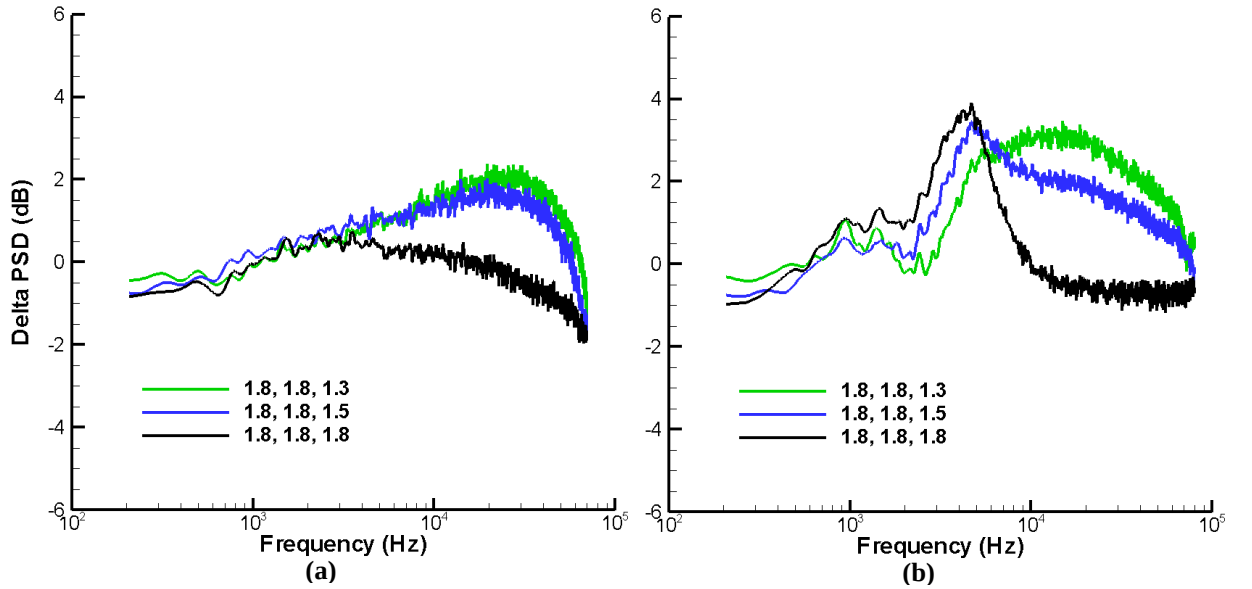

Figure 6. Power-spectral-density level differences obtained by subtracting the levels obtained at the indicated jet conditions from those obtained at the same core and bypass conditions and NPR_t = 1.0. The data were acquired for NTR_c = 3.2, and M_{fj} = 0. The observation angles are (a) 90° and (b) 150°.

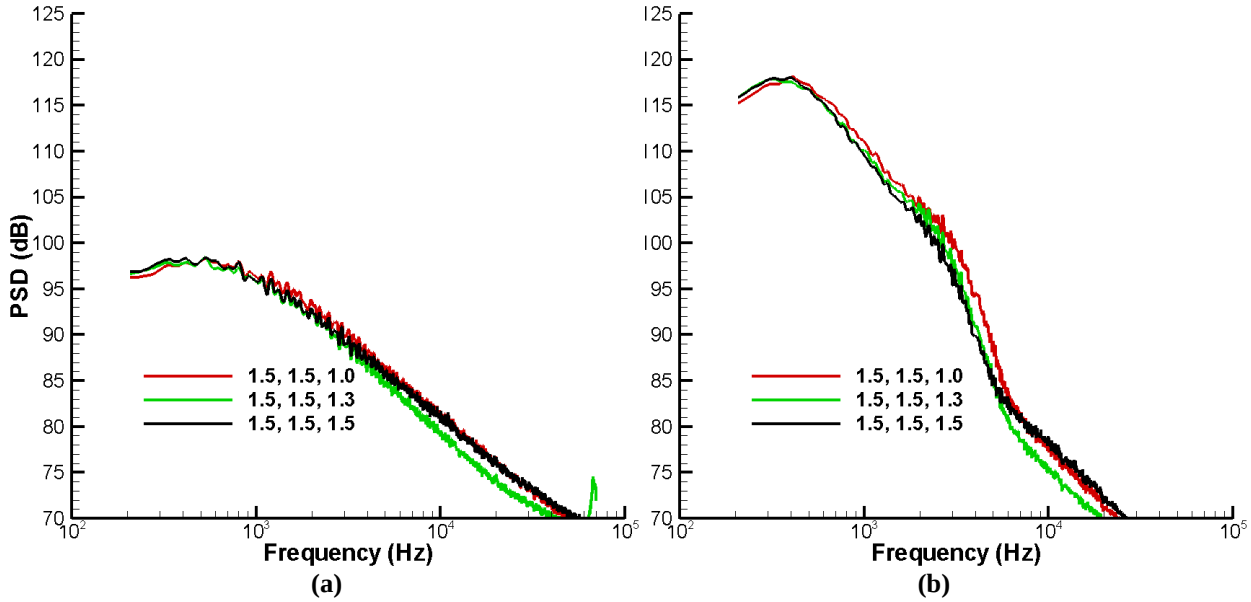

Figure 7. Narrowband data acquired at NTR_c = 3.2, M_{fj} = 0, and the indicated NPRs for observation angles equal to (a) 90° and (b) 150°.

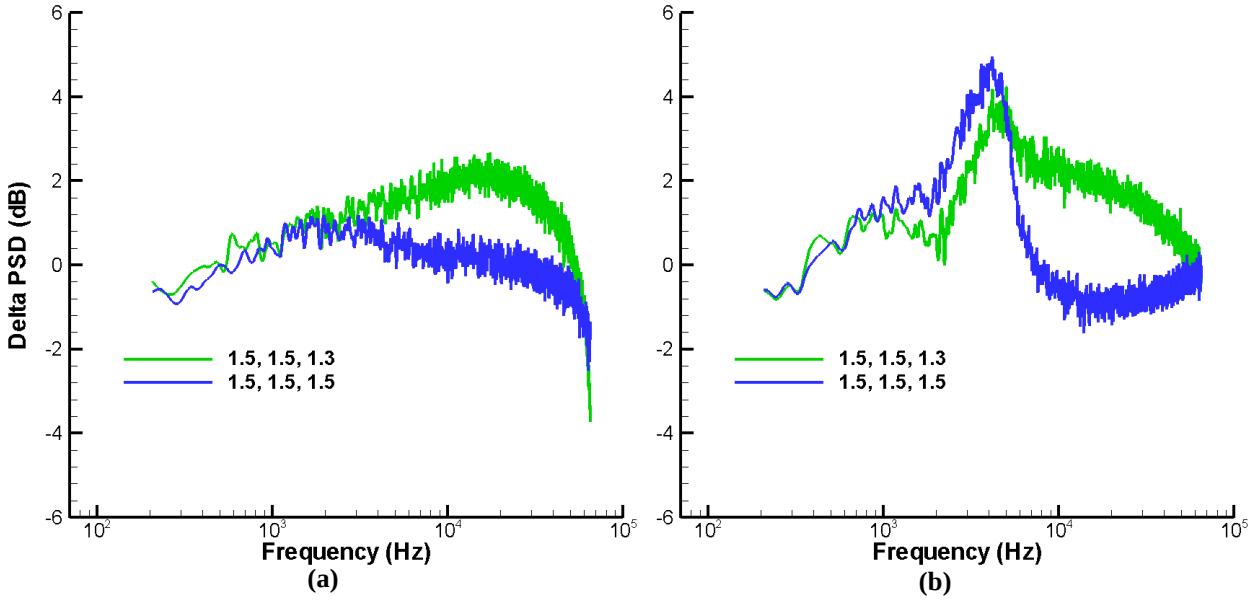

Figure 8. Power-spectral-density level differences obtained by subtracting the levels obtained at the indicated jet conditions from those obtained at the same core and bypass conditions and NPR_t = 1.0. The data were acquired for NTR_c = 3.2, and M_{fj} = 0. The observation angles are (a) 90° and (b) 150°.

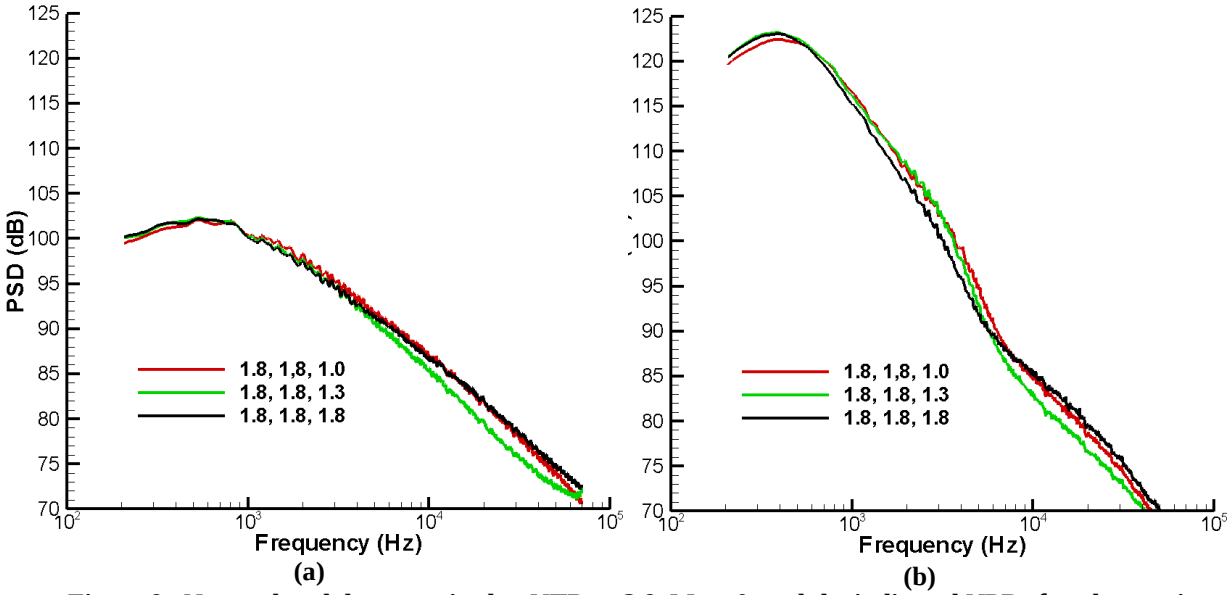

Figure 9. Narrowband data acquired at NTR_c = 2.8, M_{fj} = 0, and the indicated NPRs for observation angles equal to (a) 90° and (b) 150°.

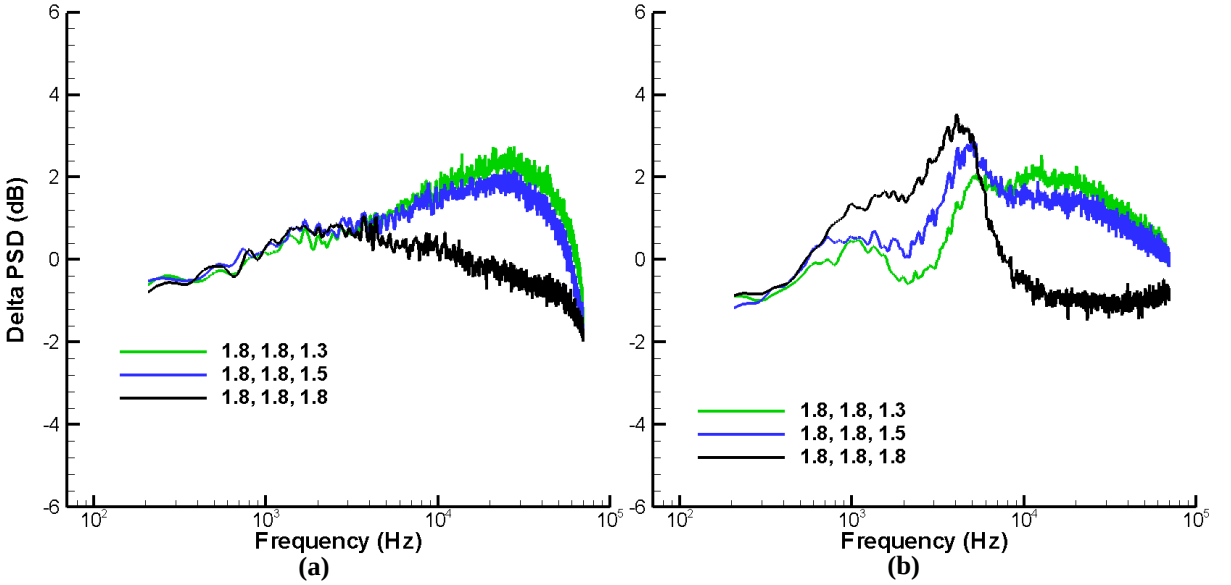

Figure 10. Power-spectral-density level differences obtained by subtracting the levels obtained at the indicated jet conditions from those obtained at the same core and bypass conditions and NPR_t = 1.0. The data were acquired for NTR_c = 2.8, and M_{fj} = 0. The observation angles are (a) 90° and (b) 150°.

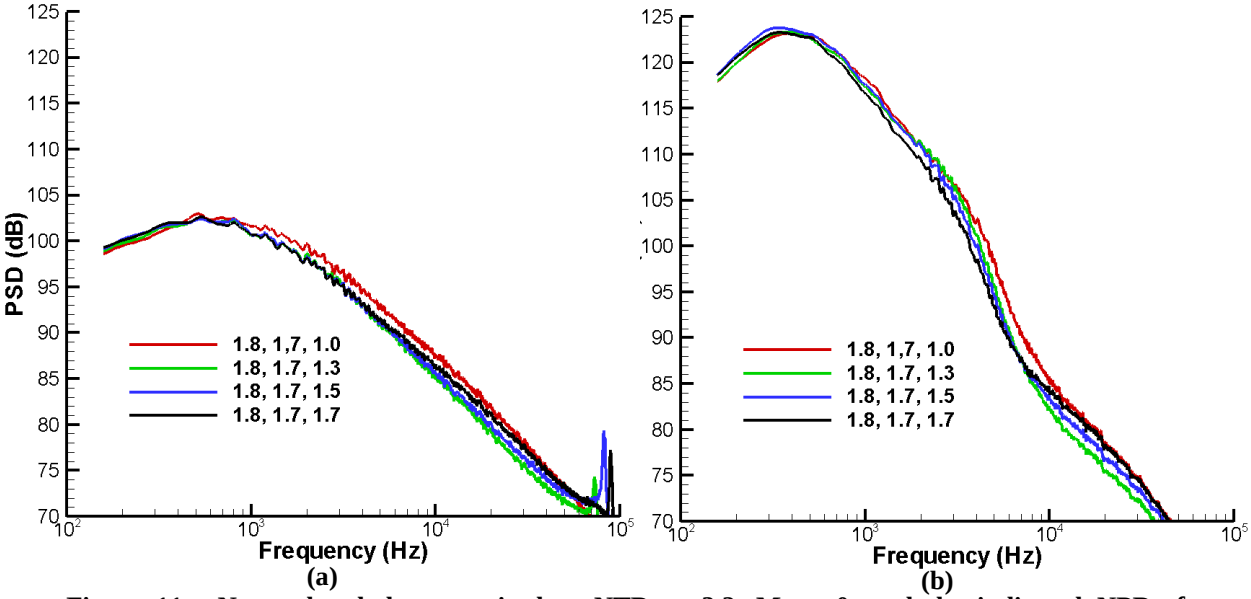

Figure 11. Narrowband data acquired at NTR_c = 3.2, M_{fj} = 0, and the indicated NPRs for observation angles equal to (a) 90° and (b) 150°.

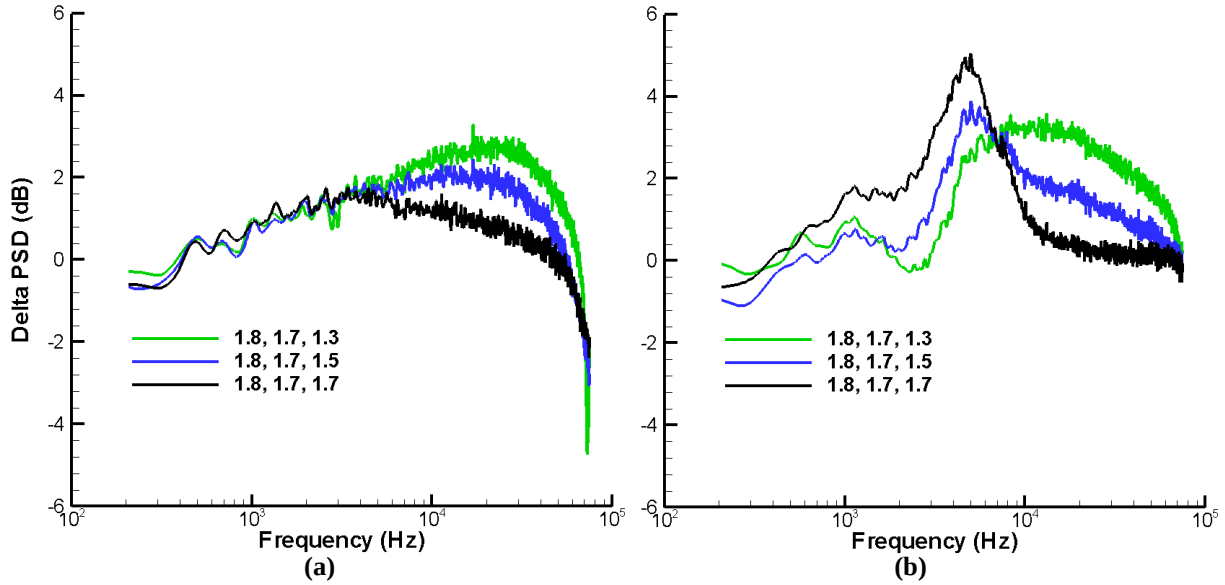

Figure 12. Power-spectral-density level differences obtained by subtracting the levels obtained at the indicated jet conditions from those obtained at the same core and bypass conditions and NPR_t = 1.0. The data were acquired for NTR_c = 3.2, and M_{fj} = 0. The observation angles are (a) 90° and (b) 150°.

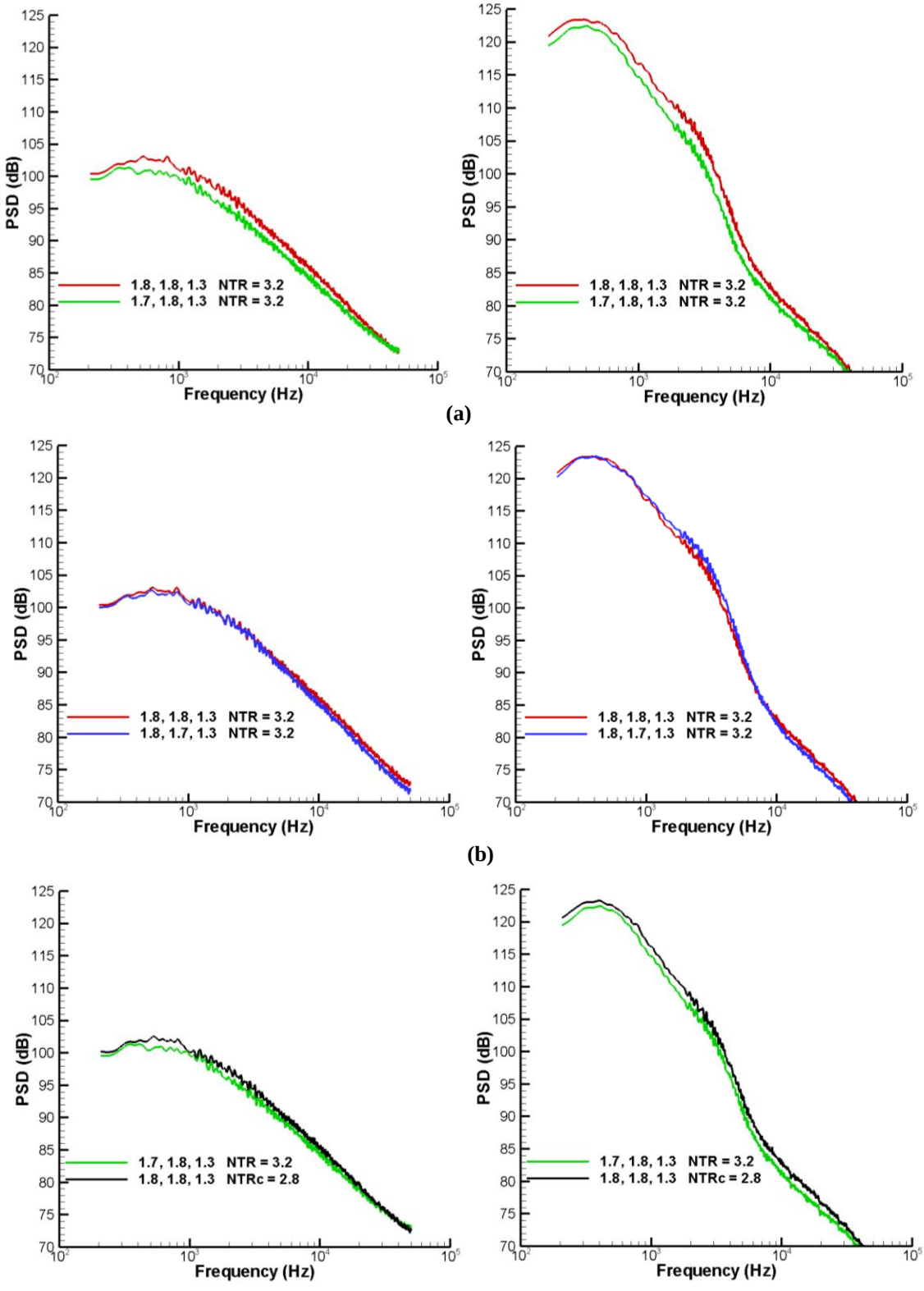

Figure 13. Narrowband data acquired at M_{fj} = 0.0, the indicated NPRs, and the indicated NTR_cs. The observation angles are 90° for the plots in column one and 150° for the plots in column two. The data show the impact of (a) reduced core velocity, (b) reduced bypass velocity, and (c) reduced bypass-to-core mass-flow ratio on radiated noise.

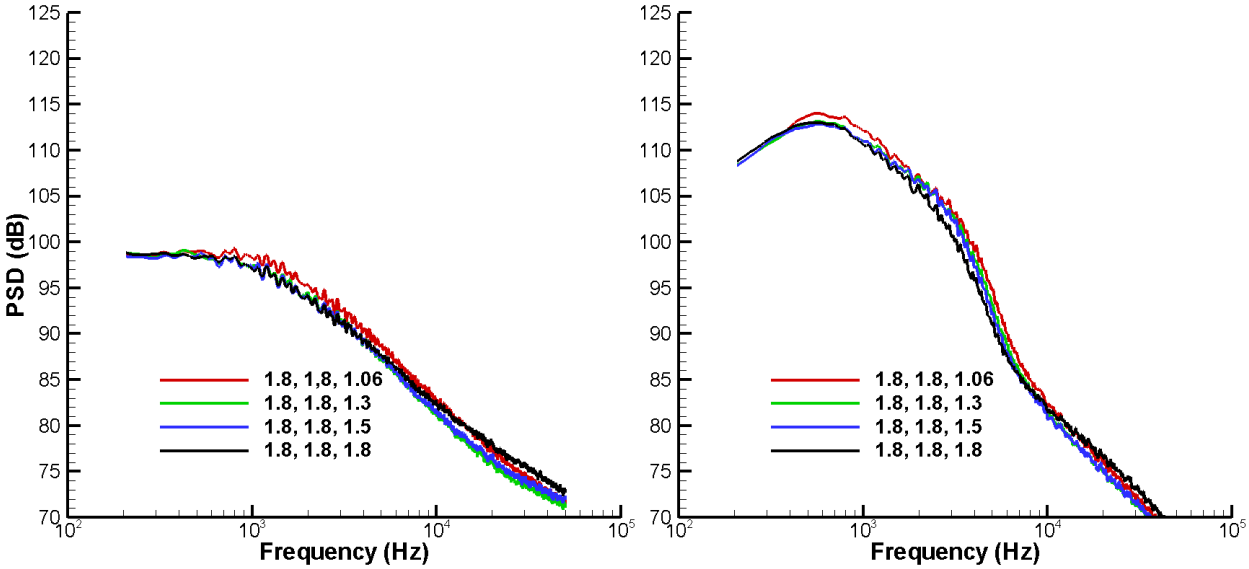

Figure 14. Narrowband data acquired at NTR_c = 3.2, M_{fj} = 0.3, and the indicated NPRs for observation angles equal to (a) 90° and (b) 150°.

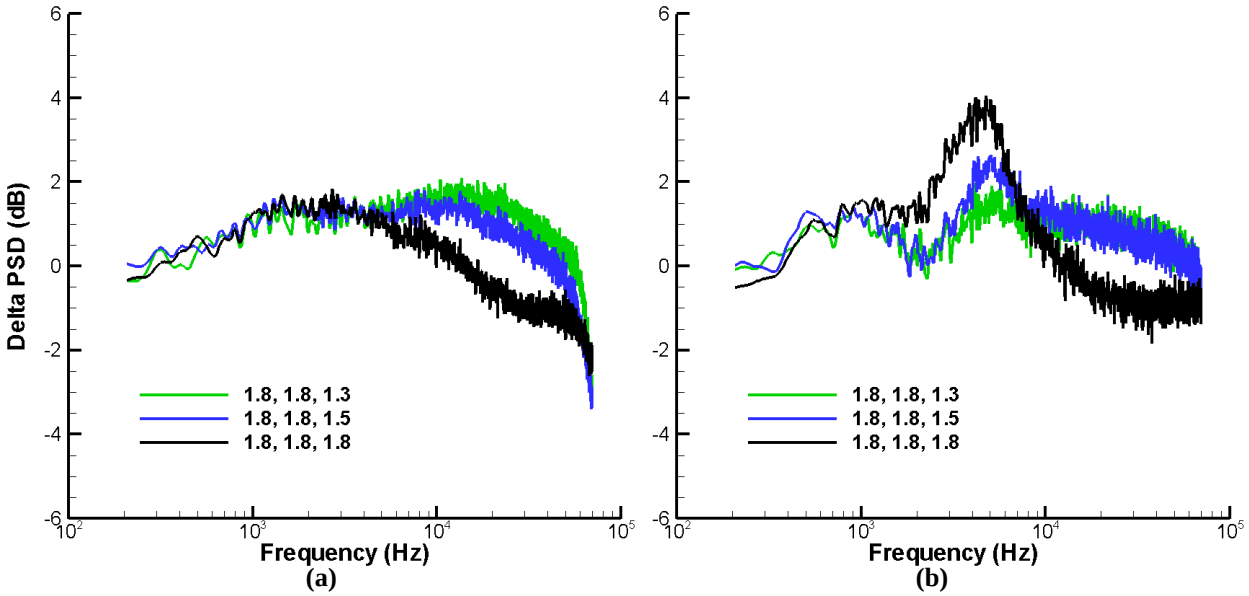

Figure 15. Power-spectral-density level differences obtained by subtracting the levels obtained at the indicated jet conditions from those obtained at the same core and bypass conditions and NPR_t = 1.0. The data were acquired for NTR_c = 3.2, and M_{fj} = 0.3. The observation angles are (a) 90° and (b) 150°.

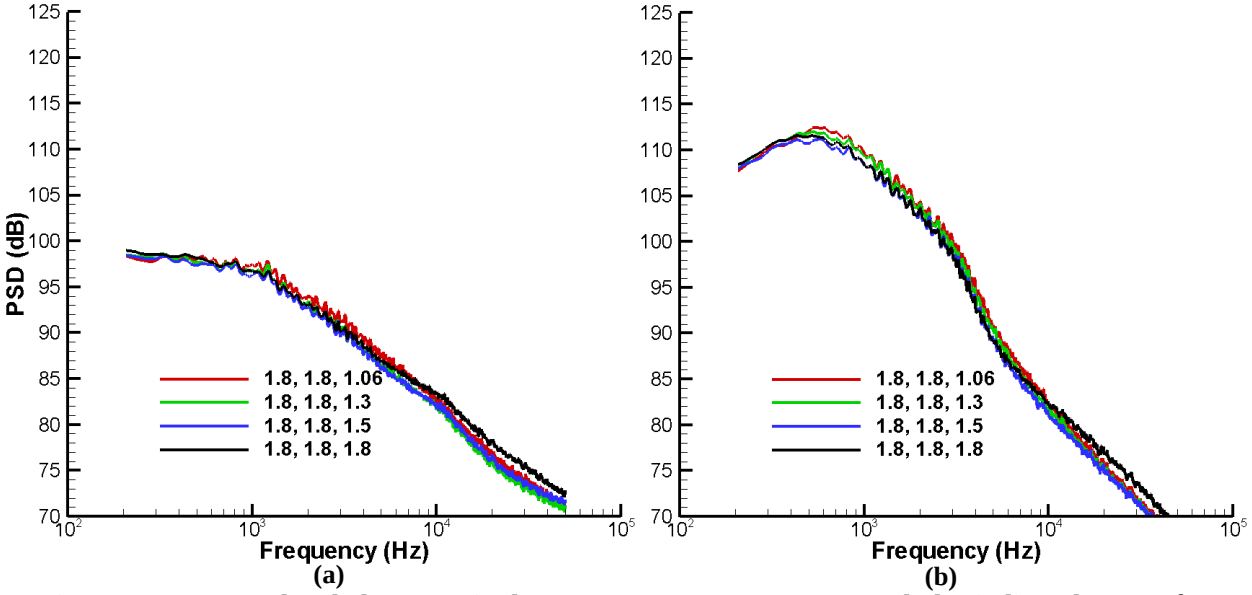

Figure 16. Narrowband data acquired at NTR_c = 3.2, M_{fj} = 0.3, and the indicated NPRs for observation angles equal to (a) 90° and (b) 150°. The core lobed mixer was used in these experiments.

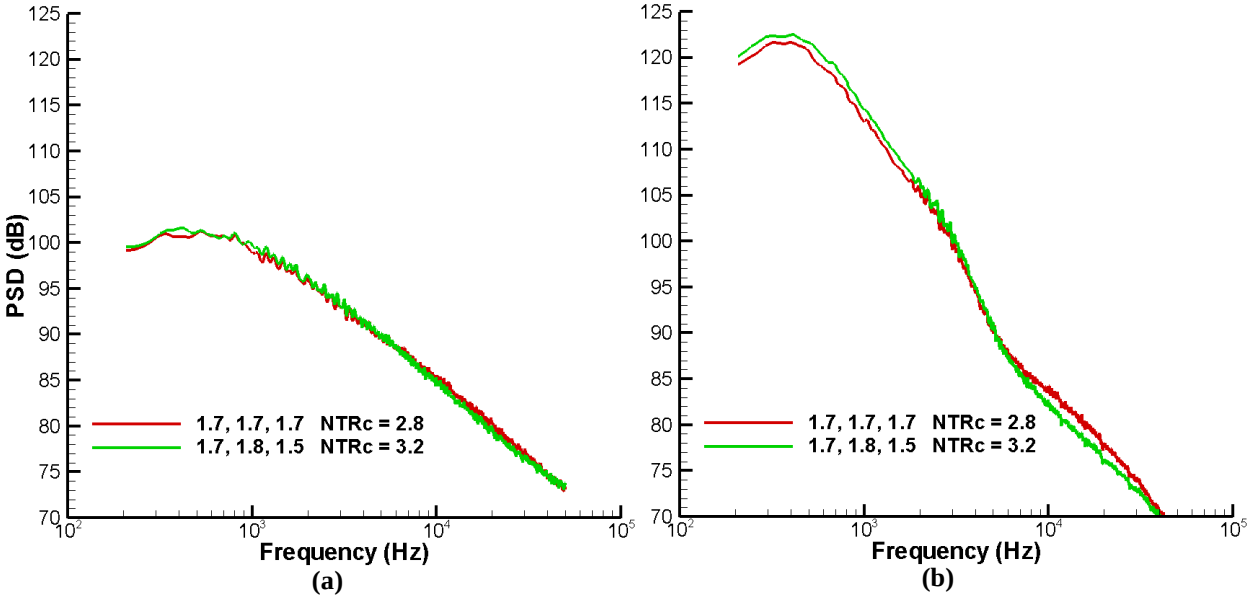

Figure 17. Narrowband data acquired M_{fj} = 0, the indicated NPRs, and the indicated NTR_cs for observation angles (a) equal to 90° and (b) in the peak jet noise direction. The data were acquired for equal ideal thrust.

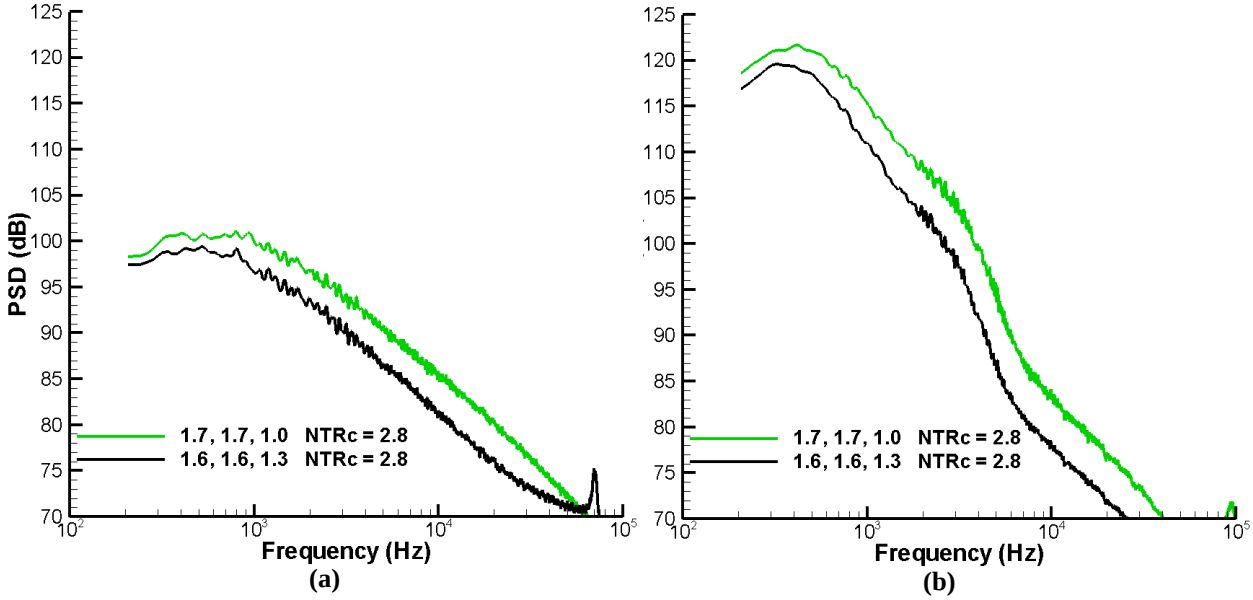

Figure 18. Narrowband data acquired M_{fj} = 0, the indicated NPRs, and the indicated NTR_cs for observation angles (a) equal to 90° and (b) in the peak jet noise direction. The data were acquired for equal ideal thrust.